An Oxide Semiconductor Nanoparticle in an Aqueous Medium: A Surface Charge Density Investigation

Fanyao Qu[†] and Paulo Cesar Morais*

Universidade Federal de Uberlândia, Departamento de Ciências Físicas, Laboratório de Novos Materiais Isolantes e Semicondutores, CEP 38400-902, Uberlândia-MG, Brazil and Universidade de Brasília, Instituto de Física, Núcleo de Física Aplicada, C.P. 04455, CEP 70919-970, Brasília-DF, Brazil

Received: October 25, 1999; In Final Form: February 5, 2000

The surface charge density in semiconductor metal oxide quantum dots dispersed in alkaline aqueous colloids was obtained by solving the three-dimensional Schrödinger and Poisson's equations. The calculation was carried out self-consistently within the frame of the finite difference method. Surface charge density, in the range of 0.1−0.3 C/m^2, was obtained for spherical ZnO nanoparticles in an aqueous medium at pH around 11. The calculated surface charge density, in very good agreement with the average value reported in the literature (0.2 C/m^2), is obtained as long as a proton-transfer mechanism through the semiconductor−electrolyte interface takes place. The calculated band energy profile for water-based semiconductor colloidal quantum dots, is very much similar to the band energy profile found in symmetric modulation-doped semiconductor quantum wells.

1. Introduction

The problem of charging and discharging semiconductor quantum dots (QDs) with electric charge in a controlled way has been the focus of intense basic and technological investigation in the last two decades.[1] The modulation-doped quantum dot (MDQD) would not require any electric contact to be charged and discharged because electric charge can be transferred out from the quantum structure by laser illumination.[2] Likewise, positively or negatively charged metal oxide (M_xO_y) semiconductor QDs may be suspended in water to form stable colloids. Such colloids are useful in photonics,[3] environment cleanup,[4] and *in vitro* cell separation,[5] among many other applications. In contrast to MDQD, where the optical-induced charge-transfer mechanism is well-established at zero[6] and nonzero[7] magnetic fields, the charging of M_xO_y semiconductor QDs suspended in water is controversial.[8−10] The band gap of a semiconductor metal oxide spans a wide range of values, as for instance, VO (0.3 eV), FeO (2.0 eV), TiO_2 (3.0 eV), Fe_2O_3 (3.1 eV), and ZnO (3.2 eV).[11] The net positive or negative charge in a nanoparticle will be accommodated in the quantum-confined subbands of the valence band or conduction band, respectively. The subbands, however, are very sensitive to the nanoparticle size, effective mass, band offset at the semiconductor−solvent interface, and counterion concentration. Note that negatively charged M_xO_y nanoparticles yield stable colloids in alkaline medium (pH > 8), whereas positively charged nanoparticles account for stable colloids in acid medium (pH < 6).[12] The negative charge developed in a metal oxide nanoparticle is assumed to be due to partially bonded oxygen atoms (M−O−) at the nanoparticle surface.[13] The neutral hydroxyl group bonded at the nanoparticle surface (M−OH) also plays a very important role in the chemical equilibrium involving the positively or negatively charged nanoparticle.[14] In addition, it is assumed here that negative charge is build up on the aqueous dispersed nanoparticle due to proton (H^+) transfer out from the nanoparticle surface toward the solvent. Thus, when starting at the zero point of charge and increasing the pH value in the aqueous medium, the chemisorbed proton (H^+) is assumed to jump out from the nanoparticle surface (M−OH), leaving behind the electron in the partially bonded oxygen atom (M−O−). The electron left behind would be accommodated in the nanoparticle conduction band while the surface oxygen atom is stabilized by a strongly bonded water layer around the nanoparticle surface.[15] Such a proton-transfer mechanism sets in a negative charge, which is mainly localized at the nanoparticle surface. In contrast, when starting at the zero point of charge and lowering the pH in the aqueous medium, the available protons (H^+) are assumed to transfer from the acid solvent back to the nanoparticle surface, thus setting up a positive charge at the nanoparticle surface (M−OH_2^+).[13] Therefore, the charge−discharge process of an M_xO_y semiconductor QD in aqueous solution is assumed to involve proton (H^+) transfer through the strongly bonded water layer of thickness (L_S-L_W) at the M_xO_y/H_2O interface (see Figure 1). One point, however, deserves special attention, namely, the typical value of the effective mass of the carrier in the barrier ($m_B = 140$). Such a huge effective mass in the barrier corresponds to the proton (H^+), which transfers into the QD and out from the QD toward the solvent through the strongly bonded water layer of thickness (L_S-L_W). In the present work, a semiconductor band profile for charged M_xO_y semiconductor QDs suspended in water is proposed which gives excellent results for the surface charge density, as compared to the values obtained by chemical methods[16] and by magnetic resonance experiments.[17] The QD surface charge density is calculated as a function of the band offset at the semiconductor−electrolyte interface and as a function of the QD size at pH 11.5.

2. Theory

The schematic energy band diagram, proposed for an isolated spherical M_xO_y semiconductor QD immersed in alkaline aqueous

* To whom correspondence should be addressed at the Universidade de Brasília. Tel.: (+55) 61-2736655. Fax: 61-2723151. E-mail: pcmor@fis.unb.br.

[†] Universidade Federal de Uberlândia.

10.1021/jp993783n CCC: $19.00
Published on Web 05/12/2000

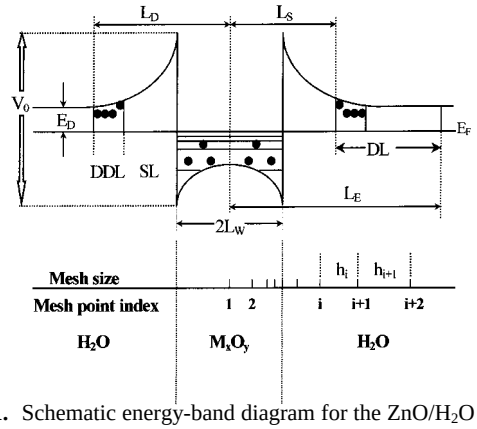

Figure 1. Schematic energy-band diagram for the ZnO/H_2O QD. The discretization of the potential based on a nonuniform mesh is schematically represented as well.

solution (negatively charged QD), is shown in Figure 1. Note that the nanoparticle diameter is given by $2L_W$, the spacer layer (SL) thickness is (L_S-L_W), the donor depletion layer (DDL) thickness is (L_D-L_S), and the donor layer (DL) thickness is (L_E-L_S). The confined bound states inside the QD are described by $E_{n,l}$ ($n,l = 0, 1, 2, ...$). E_D is the donor ionization energy, and V_0 is the band offset. As obtained from magnetic resonance measurements, in aqueous charged colloids the SL is typically one nanometer thick and is assumed to be due to water molecules strongly bonded at the nanoparticle surface.[17] In alkaline aqueous colloids, the DDL about the nanoparticle corresponds to the region where the positively charged counterions are distributed.[18] The DDL is an ionized layer, and from the microscopic point of view, the electric charge neutrality holds as long as the nanoparticle is included in the region under consideration. The band offset value (V_0) represents the difference between the chemical potential at the band edge of the nanoparticle (M_xO_y) and the chemical potential of the pure solvent (H_2O). Experimental data obtained from M_xO_y semiconductors in aqueous media indicates that V_0 goes typically up to 1 eV,[19] being very sensitive to the pH value.[20] The M_xO_y nanoparticle dispersed in water solution is now treated as a spherically symmetric M_xO_y/H_2O QD. The QD electronic structure is then obtained numerically by solving self-consistently the Schrödinger and Poisson's equations in the frame of the finite-difference method (FDM) with a nonuniform mesh size.[21]

Electronic states in spherical, negatively charged, semiconductor QD could be described by a single-electron one-band effective mass approximation[22]

$$\left[-\frac{1}{2}\nabla\left(\frac{1}{m(r)}\nabla\right) + U(r)\right]R_{n,l}(r)Y_{l,m}(\theta,\phi) = ER_{n,l}(r)Y_{l,m}(\theta,\phi) \quad (1)$$

where $R_{n,l}(r)$ is the radial part of the envelope function, with n and l meaning the principal and orbital quantum numbers, respectively. $Y_{l,m}(\theta,\phi)$ is the lth order spherical harmonic basis function, with θ and ϕ being the polar and azimuthal angles of the wave vector, respectively. $U(r) = V_0 + V_H$ is the local potential, where V_0 is the conduction band offset and V_H is the Hartree potential. Throughout this work, effective atomic units will be used, whereby the units of length, energy and mass are respectively $a_B = \epsilon_0\hbar^2/m_0e^2 = 0.529$ Å, $R_Y = \hbar^2/m_0a_B^2 = 27.212$ eV, and m_0. The electron mass, elementary charge, and permittivity of free space is m_0, e, and ϵ_0, respectively. The radially dependent relative mass is given by $m(r) = m_W$ (m_B) for $r < L_W$ ($r \geq L_W$), where $m_W = m_W^*/m_0$ and $m_B = m_B^*/m_0 \cdot m_W^*$ and m_B^* are, respectively, the effective mass of the carrier in the QD (M_xO_y) and in the barrier (H_2O). Introducing the new function $\psi_{n,l}(\lambda,r)$, with $R_{n,l}(r) = \psi_{n,l}(\lambda,r)/r$, eq 1 can be written

$$\frac{1}{2m(r)}\frac{d^2\psi_{n,l}(\lambda,r)}{dr^2} - U_{EFF}(r)\psi_{n,l}(\lambda,r) = \lambda\psi_{n,l}(\lambda,r) \quad (2)$$

with $U_{EFF}(r) = U(r) + l(l+1)/2m(r)r^2$. $U(r)$ is the local potential, and λ is related to the energy ($\lambda = -E$). The self-consistent Hartree potential V_H satisfies Poisson's equation

$$\epsilon(r)\nabla^2V_H = [n_D(r) - n(r)] \quad (3)$$

where $\epsilon(r)$ is the radially dependent dielectric constant of the material, given by $\epsilon(r) = \epsilon_W$ (ϵ_B), for $r < L_W$ ($r \geq L_W$). ϵ_W and ϵ_B are the dielectric constants of M_xO_y and H_2O, respectively. The charge density (n) and ionized donor concentration (n_D) are described respectively by

$$n(r) = \frac{1}{2\pi}\sum_{l=0}^{l_{max}}(2l+1)\sum_{n=1}^{N_T}|R_{n,l}|^2f_{FD}(E_{i,l}) \quad (4)$$

and

$$n_D(r) = \begin{cases} \dfrac{N_D}{1 + 2\exp\{[E_F - E_D(r)]/kT\}} & L_S \leq r \leq L_D \\ 0 & \text{otherwise} \end{cases} \quad (5)$$

where E_F is the Fermi energy and $\int_0^\infty[R_l(r)]^2r^2dr = 1$. N_D is the donor concentration, $E_D(r) = E_D + U(r)$ is the donor ionization energy, and f_{FD} is the Fermi−Dirac distribution function. The sum in eq 4 has to be performed over all occupied electronic states. The Fermi level (E_F) at $r \rightarrow L_E$ coincides with the donor level located at energy E_D below the conduction band (see Figure 1). The energy reference level is chosen as the conduction band edge of the zero-charged QD.

Introducing the new function ϕ_H through $V_H = \phi_H/r$, eq 3 reads

$$\epsilon(r)\frac{d^2\phi_H}{dr^2} = r[n_D(r) - n(r)] \quad (6)$$

At the interface QD/SL, the Hartree self-consistent potential and its first derivative are continuous due to the Gauss law. At the center of the QD ($r = 0$), ϕ_H is chosen as zero, that is, $\phi_H(r = 0) = 0$. The global charge neutrality of the structure implies that $\int_0^\infty[n(r) - n_D(r)]r^2dr = 0$. Using the charge density expression, one obtains

$$\int_0^\infty n(r)r^2dr = \frac{1}{2\pi}\sum_{l=0}^{l_{max}}(2l+1)\sum_{n=1}^{N_T}f_{FD}(E_{i,l}).$$

To solve numerically the coupled Schrödinger and Poisson's equations, discretization of eqs 2 and 6 are performed using the three-point finite-difference scheme (see Figure 1). The index i identifies the grid point on the one-dimensional mesh. To take the mesh size h_i as nonuniform and thus take full advantage of the computational simplifications resulting from matrix symmetry, the parameter $L_i^2 = (h_i + h_{i-1})/2$ is defined. The Schrödinger equation is then cast as a matrix equation

$$\sum_{j=1}^{NT} A_{ij}\psi_j = \lambda\psi_i \tag{7}$$

where

$$A_{ij} = \begin{cases} \frac{1}{2m_W}\frac{2}{h_i L_i^2} & ; j = i+1 \\ \frac{1}{2m_W}\frac{2}{h_{i-1} L_i^2} & ; j = i-1 \\ -(A_{ij+1} + A_{ij-1} + U_{EFF}^i) & ; j = i \\ 0 & ; \text{otherwise} \end{cases} \tag{8}$$

for points inside the QD and

$$A_{ij} = \begin{cases} \frac{1}{2m_B}\frac{2}{h_i L_i^2} & ; j = i+1 \\ \frac{1}{2m_B}\frac{2}{h_{i-1} L_i^2} & ; j = i-1 \\ -(A_{ij+1} + A_{ij-1} + U_{EFF}^i) & ; j = i \\ 0 & ; \textit{otherwise} \end{cases} \tag{9}$$

for points in the barrier. Likewise, Poisson's equation takes the following matrix form:

$$\sum_{j=1}^{NT} C_{ij}\phi_{Hj} = \rho_i^{(EFF)} \tag{10}$$

where $\rho^{(EFF)}(r) = r[n_D(r) - n(r)]$ and

$$C_{ij} = \begin{cases} \epsilon_W\frac{1}{h_i L_i^2} & ; j = i+1 \\ \epsilon_W\frac{1}{h_{i-1} L_i^2} & ; j = i-1 \\ -(C_{ij+1} + C_{ij-1}) & ; j = i \\ 0 & ; \textit{otherwise} \end{cases} \tag{11}$$

for points inside the QD. For points in the barrier, however, C_{ij} is given by

$$C_{ij} = \begin{cases} \epsilon_B\frac{1}{h_i L_i^2} & ; j = i+1 \\ \epsilon_B\frac{1}{h_{i-1} L_i^2} & ; j = i-1 \\ -(C_{ij+1} + C_{ij-1}) & ; j = i \\ 0 & ; \textit{otherwise} \end{cases} \tag{12}$$

The self-consistent calculation procedure uses an initial guess for the Hartree potential V_H. We chose $V_H = \gamma \times r^2$ in the region $r \le L_S$ and zero for $r > L_S$, where γ is a suitable constant. The wave functions and bound energies are then numerically computed from the Schrödinger equation, considering the initial guess for V_H. So, a new Hartree potential $V_H^{(NEW)}$ is then calculated by numerically solving Poisson's equation and is compared to the previous one ($V_H^{(OLD)}$) through

$$\mu = \frac{\int dr|V_H^{(NEW)} - V_H^{(OLD)}|}{\int dr V_H^{(OLD)}} \tag{13}$$

If μ is larger than some specified tolerance, the new Hartree potential is then mixed with the old one according to $V_H = (1 - f)V_H^{(OLD)} + fV_H^{(NEW)}$, with $0 < f < 1$. The mixed Hartree potential is used as an input to the calculation, and this procedure is iterated until μ becomes smaller than the tolerance. In other words, convergence is achieved when the previous Hartree potential and the new one do not vary much.

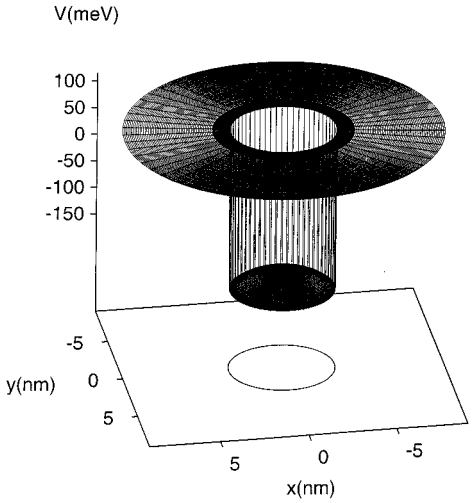

Figure 2. Potential energy as function of position, for $V_0 = 300$ meV, $L_W = 3.0$ nm, $m_W = 0.24$, $L_S = 4.0$ nm and $\epsilon_W = 3.7$.

3. Results and Discussions

Numerical calculation was performed for the negatively charged (alkaline medium) ZnO/H_2O spherical QD. The following parameters were used in the calculation: $L_S - L_W = 1.0$ nm, $L_D = 18$ nm, $L_E = 20\ L_W$, $E_D = 50$ meV, $m_B = 140$, $\epsilon_B = 80$, $m_W = 0.24$, $\epsilon_W = 3.7$, $N_D = 1.8 \times 10^{18}/cm^3$, and $T = 300$ K. The N_D value ($1.8 \times 10^{18}/cm^3$) corresponds to pH 11.5. The QD size (L_W) corresponds to a few nanometers, whereas the band offset (V_0) spans from 0.35 to 0.80 eV. Figure 2 shows the typical potential energy as a function of radial position. Note that the schematic representation of the energy band diagram (see Figure 1) is in excellent agreement with a cross section of the three-dimensional representation of the calculated potential energy, as shown in Figure 2. It is found that the band-bending occurs in the form of the Hartree self-consistent potential, decreasing with the distance from the center of the QD structure. The QD potential energy reaches its minimum value at the ZnO/H_2O interface. The electron probability for the ground state as well as for the first excited state vary slowly inside the QD, becoming very steep near the ZnO/H_2O interface, thus resulting in a zero-dimensional electron gas (0DEG).[22]

To systematically study the effect of the zero-dimensionality as well as the QD charge process, the density of the 0DEG was self-consistently calculated. We found that the 0DEG starts with a finite value at the center of the QD and increases to the maximum value as one moves toward the ZnO/H_2O interface, following a rapid decrease down to zero at the H_2O spacer layer. Therefore, electrons in the QD tend to stick at the ZnO/H_2O interface. The surface charge density (σ) at the ZnO/H_2O interface was calculated using the following expression

$$\sigma = 2\sum_{l=0}^{l_{max}}\sum_{n=1}^{N_T}(2l+1)f_{FD}(E_{i,l})\int_0^{L_W}|R_{n,l}(r)|^2 r^2 dr \tag{14}$$

where the sum is over all occupied electronic states (n,l). The factor 2 accounts for the spin degeneracy. Figure 3 shows the surface charge density versus conduction band offset (V_0) for

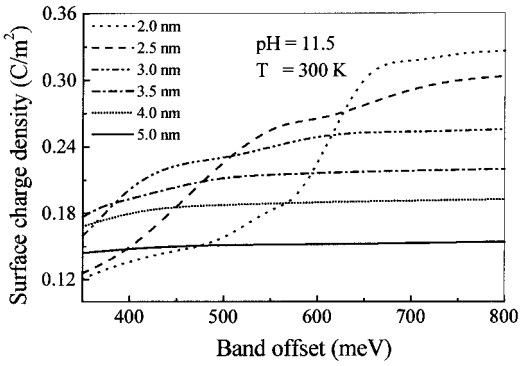

Figure 3. The electron surface charge density versus the conduction band offset, for different ZnO particle size values (L_W = 2.0, 2.5, 3.0, 3.5, 4.0, and 5.0 nm) immersed in alkaline aqueous solution.

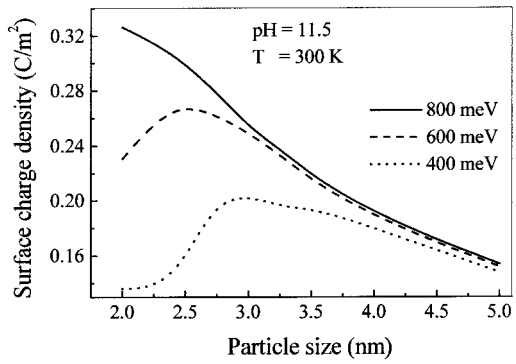

Figure 4. The electron surface charge density versus the particle size, for different ZnO conduction band offset values (V_0 = 400, 600, and 800 meV) immersed in alkaline aqueous solution.

different QD sizes. Note the excellent agreement between the range of the calculated surface charge density values shown in Figure 3 (0.1−0.3 C/m^2) and the typical value found in the literature (around 0.2 C/m^2), using techniques as different as protometric and conductometric titration[16] and magnetic resonance measurements.[17] It has been found that for small-sized nanoparticles (L_W = 2.0 and 2.5 nm) the surface charge density increases as a function of the conduction band offset, with a pronounced upshift in the 350−550 meV band offset range for L_W = 2.0 nm. For L_W = 2.5 nm, however, the surface charge density upshift occurs in the 500−650 meV band offset range. For intermediate-sized nanoparticles (L_W = 3.5 and 4.0 nm), the surface charge density increases slowly with the increasing of the conduction band offset. However, for large-sized nanoparticles (L_W = 5.0 nm), the surface charge density shows a flat behavior as a function of the band offset.

Figure 4 displays the QD size dependence of the surface charge density of ZnO nanoparticles for three different conduction band offset values. The solid, dashed, and dotted lines correspond to V_0 = 800, 600, and 400 meV, respectively. Different band offset values in Figure 4 lead to different results for the surface charge density. For the highest band offset value (V_0 = 800 meV), the surface charge density increases monotonically with the decreasing of the QD size. However, for the moderate (V_0 = 600 meV) and small (V_0 = 400 meV) band offset values, the surface charge density peaks at a particular QD size. The surface charge density first increases as the QD size decreases from higher values, reaching a peak value at a well-defined QD size, following a decrease as the QD size approaches zero. The curve peak in Figure 4 shifts to the right as the QD size decreases. The peak in the curve of the surface charge density versus QD size is a signature of the smooth transition from a three-dimensional to a zero-dimensional behavior. Note in Figure 4 that large surface charge density differences, due to differences in the band offset values, are observed in small QDs. However, wider QDs display minor differences in the surface charge density as the band offset is changed. In addition, for a particular QD size, it is also noted that the higher the band offset values, the larger the surface charge density.

The main features observed in Figures 3 and 4 are due to two effects. The first is the quantum confinement effect in the QD region, provided by the conduction band offset value and strongly affected by the QD size. In fact, as the QD size decreases, the carrier wave function is initially compressed, thus leading to the enhancement of the surface charge density. Below a certain QD size value, however, the leakage of the wave function out of the QD toward the barrier region becomes more significant. As a consequence of the wave function leakage, the surface charge density starts to decrease as the QD size reduces. Note that the leakage of the wave function becomes more efficient as the band offset reduces. The second effect is played by the donor centers located in the barrier region. Note that the bound states inside the QD are calculated with respect to the conduction band edge of the zero-charged QD, whereas the donor ionization energy is quoted with respect to the band edge of the barrier material. Therefore, before any charge is transferred between the QD and the donor centers, the system faces a very unstable situation, for the chemical potentials inside and outside the QD do not match each other. To establish the thermodynamic equilibrium, charge-transfer between the QD and the donor center takes place, driven by thermal effects. However, the charge-transfer mechanism leading to the thermodynamic equilibrium strongly depends on the conduction band offset. For narrow QDs, the charge-transfer mechanism is very sensitive to the band offset value and becomes more efficient as the band offset increases from 400 to 800 meV (see Figures 3 and 4). In other words, for narrow QD, the first bound state inside the QD as well as the Fermi level are efficiently pushed up in energy as the quantum confinement (band offset) increases, thus favoring the transfer-of-charge mechanism.[22] Therefore, the surface charge density increases, although the penetration of the QD wave function into the barrier is reduced. In contrast, in wider QDs the charge-transfer mechanism depends weakly on the conduction band offset, as shown by both the presence of a wide flat region in the curves of Figure 3 (for L_W > 3.5 nm) and by the merging of the curves of Figure 4 (for L_W > 4.0 nm).

4. Conclusion

The self-consistent procedure for calculating the band energy profile and surface charge density in metal oxide semiconductor quantum dots dispersed in aqueous solution, in the frame of the finite-difference method with a nonuniform mesh size, is presented. The use of the proper algebraic transformation allows the complicated three-dimensional Schrödinger and Poisson's equations to be written in suitable forms, which are easily used within the finite-difference method. This method is very efficient in finding eigenstates extending over relatively large spatial areas without loss of accuracy. The surface charge density obtained for metal oxide semiconductor quantum dots immersed in a water medium, at typical band offset values (0.35−0.80 eV), falls in the range of the experimental values reported in the literature (around 0.2 C/m^2). Finally, the calculation indicates that the proton (H^+) transfer mechanism through the potential barrier around the metal oxide QD immersed in water solution

takes place. Such a proton-transfer picture may represent the key to understanding the very details of the negative and positive charging mechanism of water-based colloidal nanoparticles.

Acknowledgment. This work was partially supported by the Brazilian agencies FAP-DF, CAPES, and CNPq.

References and Notes

(1) Chen, M.; Porod, W. *J. Appl. Phys.* **1995**, *78*, 1050.
(2) Cardoso, A. J. C.; Morais, P. C.; Cox, H. *Appl. Phys. Lett.* **1996**, *68*, 1105.
(3) Larsen, A. E.; Grier, D. G. *Nature* **1998**, *385*, 230.
(4) Forouzan, F.; Richards, T. C.; Bard, A. J. *J. Phys. Chem.* **1996**, *100*, 18123.
(5) Sestier, C.; Sabolovic, D.; Geldwerth, D.; Moumaris, M.; Roger, J.; Pons, J. N.; Halbreich, A. *Comptes Rend. Acad. Sci. Paris* **1995**, *318*, 1141.
(6) Chaves, A. S.; Penna, A. F. S.; Worlock, J. M.; Weimann, G.; Schlapp, W. *Surf. Sci.* **1986**, *170*, 618.
(7) Cardoso, A. J. C.; Qu, Fanyao; Morais, P. C. *Phys. Rev. B* **1999**, *60*, 4501.
(8) Bahnemann, D. W.; Kormann, C.; Hoffmann, M. R. *J. Phys. Chem.* **1987**, *91*, 3789.
(9) Marcus, R. A. *J. Phys. Chem.* **1990**, *94*, 1050.
(10) Lowen, H.; Madden, P. A.; Hansen, J.-P. *Phys. Rev. Lett.* **1992**, *68*, 1081.
(11) Chiang, Y.-M.; Birnie III, D.; Kingery, W. D. *Physical Ceramics: Principles for Ceramic Science and Engineering*; John Wiley: New York, 1997.
(12) Massart, R. *IEEE Trans. Magn.* **1981**, *17*, 1247.
(13) Herrmann, H.; Martin, S. T.; Hoffmann, M. R. *J. Phys. Chem.* **1995**, *99*, 16641.
(14) Chen, L. X.; Rajh, T.; Wang, Z.; Thurnauer, M. C. *J. Phys. Chem. B* **1997**, *101*, 10688.
(15) Morais, P. C.; da Silva, S. W.; Soler, M. A. G.; Sousa, M. H.; Tourinho, F. A. *J. Magn. Magn. Mater.* **1999**, *201*, 105.
(16) Bacri, J.-C.; Perzynski, R.; Salin, D.; Cabuil, V.; Massart, R. *J. Colloid Interface Sci.* **1989**, *132*, 43.
(17) Morais, P. C.; Tourinho, F. A.; Gonçalves, G. R. R.; Tronconi, A. L. *J. Magn. Magn. Mater.* **1995**, *149*, 19.
(18) Adamson, A. W. *Physical Chemistry of Surfaces*; John Wiley: New York, 1990.
(19) Rothenberg, G.; Fitzmaurice, D.; Grätzel, M. *J. Phys. Chem.* **1992**, *96*, 5983.
(20) Hoyle, R.; Sotomayor, J.; Will, G.; Fitzmaurice, D. *J. Phys. Chem.* **1997**, *101*, 10791.
(21) Todorovic, G.; Milanovic, V.; Ikonic, Z.; Indjin, D. *Phys. Rev. B* **1997**, *55*, 15681.
(22) Qu, Fanyao; Morais, P. C. *J. Chem. Phys.* **1999**, *111*, 8588.